Neutron diffraction study on structural properties of $N(CD_3)_4MnCl_3$

1996 J. Phys.: Condens. Matter 8 969

(http://iopscience.iop.org/0953-8984/8/8/008)

J. Phys.: Condens. Matter **8** (1996) 969–981. Printed in the UK

Neutron diffraction study on structural properties of $N(CD_3)_4MnCl_3$

V Rodriguez†, G Aguirre-Zamalloa†§, M Couzi† and T Roisnel‡

† Laboratoire de Spectroscopie Moléculaire et Cristalline (URA 124 CNRS), 351, cours de la Libération, Université de Bordeaux I, F-33405 Talence Cédex, France

‡ Laboratoire Léon Brillouin (CEA–CNRS), Centre d'Etudes de Saclay, F-91191 Gif sur Yvette Cédex, France

Received 19 September 1995, in final form 6 November 1995

Abstract. Crystals with formula $N(CD_3)_4MnCl_3$ (TMMC) consist of infinite linear chains, running along the c axis, composed of manganese atoms bridged by three chlorine atoms $[MnCl_3]^-$ and of disordered $[N(CD_3)_4]^+$ (TMA) located in spaces between the chains. The hexagonal structure at room temperature (space group $P6_3/m$ with $Z = 2$) is characterized by an orientational disorder of the organic group TMA. A weakly first-order phase transition occurs at 126 K which stabilizes a monoclinic low-temperature phase (space group $P2_1/b$ with $Z = 4$). The crystal structure of TMMC has been studied at 8 K and 295 K by means of powder neutron diffraction experiments. It is shown that this phase transition is characterized by an antiphase translational displacement of the infinite linear chains along the hexagonal axis which couples with an orientational ordering process of the TMA groups. This latter process can be described in the frame of a complex Frenkel model involving reorientations of the TMA groups, in the room-temperature phase, over six energetically equivalent potential wells.

1. Introduction

Tetramethylammonium manganese (II) chloride (TMMC), $N(CD_3)_4MnCl_3$, has been widely studied because of its quasi-ideal one-dimensional magnetic properties (see, e.g., [1, 2]). The crystal structure at room temperature was determined originally by Morosin and Graeber [3, 4] who found that the crystal is made of infinite linear chains of $MnCl_6$ octahedra sharing opposite faces, separated by tetramethylammonium (TMA) ions. In addition to the interesting magnetic properties of this crystal, TMMC exhibits a first-order ferroelastic structural phase transition at 126 K driven essentially by the reorientational dynamics of the TMA groups [5–14]. In the hexagonal high-temperature phase (phase I: space group $P6_3/m$ with $Z = 2$), the TMA are orientationally disordered, whereas they become progressively ordered in the low-temperature monoclinic phase (phase II: space group $P2_1/b$ with $Z = 4$). The standard setting of $P2_1/b$ is $P2_1/c$ but in this work we adopt the $P2_1/b$ description to relate more easily the high- and low-temperature structures. In such a situation, phase II corresponds to a doubling of the lattice constant along b contained in the hexagonal plane (monoclinic axis c) [5, 10, 11].

Orientational disorder in phase I arises from the incompatibility between the molecular T_d point symmetry of the free TMA and its site symmetry C_{3h} which is not a subgroup of T_d. Different models, based essentially on x-ray diffraction experiments, have been put forward. In a first model proposed by Morosin and Graeber [3], one C–N bond lies

§ Present address: Institut für Festkörperforschung KFA, D-52425 Jülich, Germany.

0953-8984/96/080969+13$19.50

on the threefold axis of the site and the TMA orientational disorder is described with a two-site model where one orientation is related to the other by the σ_h mirror plane of the site. Another possibility pointed out by Jewess [15] is that the TMA groups are not twofold disordered but threefold disordered. In this case, one mirror plane of the TMA coincides with the σ_h mirror plane of the site. Then, this leads to a three-site model for the TMA where each orientation is related to the other by the threefold axis of the site. More recently, Braud *et al* [11] concluded that an admixture of both models is necessary to obtain a satisfactory description of the electronic distribution of the carbon atoms as determined from x-ray single-crystal diffraction experiments in the disordered hexagonal phase. Attempts to determine the structure of TMMC in phase II by means of x-rays were also undertaken at 118 K, just below the transition temperature. In fact, the experimental conditions (i.e. the proximity of the phase transition, the occurrence of ferroelastic domains induced through the first-order phase transition, etc) were not favourable to determine the structure but it could be concluded that an important residual orientational disorder of the TMA is still present just below the I $\Leftrightarrow$ II transition temperature [11].

We have undertaken high-resolution neutron powder diffraction experiments in order to get a deeper insight into the nature of the phase transition. Deuterated samples, $N(CD_3)_4MnCl_3$ have been used in order to get rid of the very high incoherent neutron scattering background due to hydrogen atoms. The scope of the present study was to determine the structure of the monoclinic phase II and more precisely to get a 'frozen view' of the TMA orientation at very low temperature. Then from the knowledge of the exact position of the TMA in the ordered phase, attempts to re-interpret the disorder of the room temperature phase were carried out. Firstly, one should note that the diffracted intensity arises mainly from the $MnCl_6$ octahedra (around 90%) when using x-rays. In the case of neutron diffraction, the situation is quite different since the diffracted intensity arises mainly from the deuterated TMA groups (more than 70%). Therefore, the latter technique appears to be more powerful to clarify the orientational disorder of the organic TMA groups. Secondly, the Rietveld method is now widely recognized to be uniquely valuable for structural analyses of nearly all classes of crystalline materials not available as single crystals. As a corollary, powder diffraction experiments may also constitute a quite good approach for structural determination of samples which undergo phase transitions leading to the appearance of multidomain phases. It is noteworthy that complex twinning occurs in the low-temperature monoclinic phase of TMMC [1, 5, 11], so that a full single-crystal determination would require very good resolution measurements on one carefully selected domain. At least in a first step, neutron powder diffraction experiments seemed to be a more convenient method, TMA groups and octahedra chains behaving essentially as rigid bodies [8].

The most striking results of the present study are that the use of the Rietveld method including rigid-body constraints makes it possible to resolve low-symmetry phases with large unit cells (volume around 900 $Å^3$ for phase II of TMMC) [16] and, in addition, to investigate phases involving strong orientational disorder as is the case for the hexagonal phase I of TMMC. Indeed, it is well known that the introduction of restraints or constraints is very useful especially for the most common case which consists of rather complex structures with large unit-cell parameters and a correspondingly high degree of reflection overlap [17].

2. Experimental details

Rapid evaporation at room temperature of saturated solutions in D_2O of $N(CD_3)_4Cl$ (Interchim) and $MnCl_2$ (Merck) in stoichiometric proportions yields small pink crystalline

samples of $N(CD_3)_4MnCl_3$, which were then ground into the form of homogeneous powder.

The amount of powdered sample put in aluminium containers was chosen in order to get a transmission coefficient of about 0.9 to avoid multiple-scattering effects at small scattering angles. The neutron diffraction experiments were carried out at the Laboratoire Léon Brillouin (LLB) on the 3T2 ($\lambda = 1.23$ Å) high-resolution two-axis powder diffractometer. A standard 'orange' cryostat was used for the study at 8 K.

The data were analysed by using the program FULLPROF [18, 19]. This program allows the Rietveld refinement of multiphase patterns combining nuclear and magnetic structures. The treatment of the rigid-body constraints has been done by introducing a subroutine in which rigid-body groups of atoms or molecules can be described and constrained using internal coordinate definitions [19]. This upgraded profile fitting version of FULLPROF presents the advantage of reducing greatly the number of parameters to refine but it goes almost without saying that care must be taken when applying such constraints.

3. Structure refinement of $N(CD_3)_4MnCl_3$ in the monoclinic ordered phase at 8 K

First, it should be pointed out that the 1D–3D magnetic transition occurs at a temperature as low as 0.84 K [20, 21]; so, it can be safely stated that the diffraction pattern recorded at 8 K contains no elastic contribution from magnetic scattering [1]. In a preliminary pattern matching refinement which consisted in fitting the whole diffraction pattern using a profile model with arbitrary structure factor calculations [18, 19], 13 parameters were refined including cell parameters, profile parameters and a second-order polynomial for background refinement. Then, in early work, structural refinements were performed using rigid-body-constraints for the $MnCl_6$ octahedra and the TMA groups. The octahedra were described by means of internal coordinates for the three chlorine atoms derived from the data of Braud *et al* in the hexagonal phase [11] ($d_{Mn-Cl} = 2.564$ Å). The internal coordinates of the TMA group were those of the free molecule determined by *ab initio* calculations [22]. Hence, the organic group was supposed to be made of a perfect NC_4 tetrahedron ($d_{N-C} = 1.496$ Å) and of CD_3 methyl groups with $d_{C-D} = 1.079$ Å and $\widehat{N\text{–}C\text{–}D} = 109.04^\circ$. This early assumption for the TMA is justified since the Raman spectra of TMMC in the monoclinic phase II are consistent with nearly undistorted NC_4 tetrahedra [8]. As a matter of fact, small frequency splittings have been observed for the degenerate internal modes of the NC_4 skeleton (about 0.9% of their absolute frequencies) at low temperature [8]. Practically undistorted NC_4 tetrahedra have also been found in the structure determination of the low-temperature phase of $(CH_3)_4NCdBr_3$ (TMCB) [23].

Due to the change of origin from phase I to phase II [11] (translation of 1/4 along the b axis of the monoclinic phase), the centre of the octahedra i.e. the manganese was initially set at general position 4e (0 1/4 0) in the asymmetric unit. All the chlorines were first constrained to lie in the same horizontal plane (a, b). Moreover, the TMA group was initially centred on the latter nitrogen site 2b ($\bar{3}$) of the hexagonal phase, equivalent to a general position 4e (1/3 0.5833 1/4) in phase II. As a starting point, we chose to orientate the TMA group in an intermediate position between the two-site model and the three-site model of the disordered hexagonal phase I in such a way that two carbons C1 and C2 were located in the same vertical plane, with C1 close to the threefold axis of the hexagonal phase making an angle $z\ \widehat{\text{axis–N–C1}}$ of about 15° above the nitrogen. The other two carbons C3 and C4 lay at an initial height $z/c \approx 0.21$ i.e. in the same horizontal plane (a, b), perpendicular to the C1–N–C2 vertical plane, so as to achieve the local T_d point group symmetry of NC_4.

As the $P6_3/m \Leftrightarrow P2_1/b$ phase transition is thought to involve antiparallel translational displacements of the octahedra chains along the c direction [10–12], only two parameters for this rigid-body group were chosen to be first refined: the translation of the octahedra along c and the rotation angle about the same axis. At this stage, the TMA rigid-body group was constrained to stay along the lost hexagonal threefold axis but with three refinable orientation angles. Moreover, the angles of rotation of the four CD_3 methyls around their respective N–C axes were considered as refinable parameters. A converging process could be then performed which gave $R_{\mathrm{Bragg}} = 15\%$. The centre of mass of the two rigid-body groups rapidly shifted towards values $z/c \approx -0.05$ for the octahedra and $z/c \approx +0.27$ for the TMA. Therefore, the whole external degrees of freedom of the two rigid-body groups could be progressively refined. In a final step, the internal coordinate parameters of the octahedra and of the TMA were gradually unconstrained, i.e. conventional Rietveld refinement was finally performed, with 68 intensity-dependent parameters to describe the atomic positions in general sites 4e. The atomic temperature factors were taken to be isotropic and identical for each kind of atom (B_{D}, B_{C}, B_{N}, B_{Cl} and B_{Mn}) in consideration of the background uncertainties that can arise in such a situation where the density of Bragg peaks is so high, even at low scattering angles. After several cycles, the refinement converged to an R_{Bragg} value of 4.29%. The stability of the solution was therefore checked. The results of the neutron diffraction pattern refinement of $N(CD_3)_4MnCl_3$ at 8 K are summarized in tables 1 and 2. In figure 1 we show a plot of the observed and calculated diffraction patterns. Projections of the refined structure are reported in figures 2(a) and 2(b). Although it is well known that profile refinements of low-symmetry structures involving large unit cells can be subject to discussion, the present result seems to be rather consistent and satisfactory in the sense that the TMA groups are found practically undistorted from their ideal T_d symmetry as expected from previous Raman scattering experiments [8]. Indeed, the use of rigid-body constraints is straightforward and, in the first steps of the refinement processes, can produce physically realistic models with a large reduction in the number of adjustable parameters.

4. Tentative structure refinements of $N(CD_3)_4MnCl_3$ in the hexagonal disordered phase at 300 K

The situation in the disordered hexagonal phase I is much more complex. Several authors have tried to model the orientational disorder of the TMA in TMMC or derived compounds such as TMCB using x-ray diffraction data [2, 5, 11, 23]. Indeed as already pointed out, neutron diffraction is much more sensitive than x-rays to the position of the hydrogen (deuterium) atoms and, more generally, to the orientation of the TMA groups. As far as we know, this experiment has not yet been done. Clearly, the structure determination of the ordered monoclinic phase II is one of the keys to reconsider the nature of the orientational disorder of the TMA molecules in the hexagonal phase I.

In the light of our knowledge of TMMC [3, 5, 11], we have adopted the following procedure. The manganese atoms which occupy the centres of the octahedra are placed at the origin of the unit cell. The unique chlorine atom contained in the asymmetric unit is located in the mirror plane σ_{h} at height $z/c = 0.25$ so as to achieve the site symmetry S_6 of the octahedra. The starting coordinates in the mirror plane σ_{h} were equivalent to those of Braud *et al* [11]. The rigid undistorted TMA in the asymmetric unit was taken as described in section 3 [22] with the nitrogen atom located at special position 2c $(1/3, 2/3, 1/4)$. When comparing the diffraction patterns at 8 K and 300 K (figures 1 and 3), it can be evidenced that the high-temperature pattern induces a poorer observation/variable ratio even though peak overlapping is higher in the monoclinic phase. As a direct consequence, the R_{expected} value

Table 1. Refined parameters of $N(CD_3)_4MnCl_3$ at 8 K. The temperature factor has the form $\exp[-B\sin^2\theta/\lambda^2]$ where $B = 8\pi^2\langle u^2\rangle$. The estimated standard deviation (e.s.d.) of the last significant digit is given in parentheses. Each e.s.d. has been multiplied by a factor of 3.0 following [24].

Space group:	$P2_1/b$ ($Z = 4$)		a (Å)		8.937(4)
R_{Bragg} (%)	4.29		b (Å)		18.421(7)
R_{wp} (%)	5.60		c (Å)		6.430(3)
R_{expected} (%)	2.04		gamma (degrees)		121.282(9)
Atom	Site	x	y	z	B (Å^2)
Mn	4e	0.998(8)	0.251(4)	0.95(1)	0.4(3)
Cl(1)	4e	0.257(3)	0.333(2)	0.214(4)	0.28(6)
Cl(2)	4e	0.915(3)	0.125(2)	0.211(4)	0.28(6)
Cl(3)	4e	0.837(3)	0.289(2)	0.207(4)	0.28(6)
N	4e	0.331(3)	0.581(2)	0.276(4)	0.4(1)
C(1)	4e	0.311(5)	0.598(2)	0.502(5)	0.33(9)
C(2)	4e	0.377(5)	0.657(2)	0.153(5)	0.33(9)
C(3)	4e	0.158(4)	0.507(2)	0.211(5)	0.33(9)
C(4)	4e	0.472(4)	0.561(2)	0.261(5)	0.33(9)
D(11)	4e	0.279(5)	0.542(3)	0.590(6)	1.57(8)
D(12)	4e	0.440(5)	0.652(3)	0.550(7)	1.57(8)
D(13)	4e	0.214(5)	0.618(3)	0.507(7)	1.57(8)
D(21)	4e	0.273(5)	0.672(3)	0.163(7)	1.57(8)
D(22)	4e	0.503(5)	0.709(3)	0.199(7)	1.57(8)
D(23)	4e	0.380(5)	0.642(3)	0.992(6)	1.57(8)
D(31)	4e	0.066(5)	0.525(3)	0.215(7)	1.57(8)
D(32)	4e	0.126(5)	0.451(3)	0.304(6)	1.57(8)
D(33)	4e	0.169(5)	0.491(3)	0.051(7)	1.57(8)
D(41)	4e	0.494(5)	0.555(3)	0.099(7)	1.57(8)
D(42)	4e	0.595(5)	0.613(3)	0.328(6)	1.57(8)
D(43)	4e	0.425(5)	0.501(3)	0.338(6)	1.57(8)
Wavelength (Å)			1.2266		
Number of variables			82		
Measured reflections			2261		
Independent contributing reflections[a]			1848		

[a] Effective number of reflections accounting for refinement.

is higher in the room-temperature pattern ($R_{\text{expected}} = 5.50\%$) than in the low-temperature one ($R_{\text{expected}} = 2.04\%$). Due to this relatively poor statistics of the diffraction data at 300 K, we have chosen fixed isotropic atomic temperature factors (see table 4). It should be pointed out that we have selected Debye–Waller factors consistent with the fact that both inorganic and organic groups behave as well defined rigid-body groups where the external vibrations are largely predominant. All these conditions were kept unchanged for each orientational disorder model of the TMA presented below. The parameters to fit are always the position of the chlorine in the σ_h mirror plane, the rotations of the methyl groups about their respective N–C axis and up to three Euler angles for the whole TMA group according to the disorder description used. More details of the following refinements can be found in table 3. In any case, the refined chlorine coordinates were found to be identical within the estimated standard deviations and the carbon coordinates gave similar projections of the TMA on the (a, b) hexagonal plane.

Table 2. Selected interatomic distances (Å) and angles (degrees) of $N(CD_3)_4MnCl_3$ at 8 K. The e.s.d. of the last significant digit is given in parentheses.

Mn–Cl(1)	2.62(3)	Cl(1)–Mn–Cl(2)	80.5(7)
Mn–Cl(2)	2.64(3)	Cl(1)–Mn–Cl(3)	83.4(8)
Mn–Cl(3)	2.52(3)	Cl(2)–Mn–Cl(3)	83.2(8)
N–C(1)	1.52(2)	C(1)–N–C(2)	108(2)
N–C(2)	1.48(2)	C(1)–N–C(3)	106(2)
N–C(3)	1.49(2)	C(1)–N–C(4)	109(2)
N–C(4)	1.48(2)	C(2)–N–C(3)	111(2)
C(1)–D(11)	1.07(2)	C(2)–N–C(4)	111(2)
C(1)–D(12)	1.10(2)	C(3)–N–C(4)	112(2)
C(1)–D(13)	1.11(3)	N–C(1)–D(11)	108(2)
C(2)–D(21)	1.10(3)	N–C(1)–D(12)	109(2)
C(2)–D(22)	1.07(2)	N–C(1)–D(13)	106(2)
C(2)–D(23)	1.08(2)	N–C(2)–D(21)	111(3)
C(3)–D(31)	1.04(2)	N–C(2)–D(22)	110(2)
C(3)–D(32)	1.11(2)	N–C(2)–D(23)	107(2)
C(3)–D(33)	1.09(2)	N–C(3)–D(31)	109(3)
C(4)–D(41)	1.08(2)	N–C(3)–D(32)	110(2)
C(4)–D(42)	1.11(2)	N–C(3)–D(33)	109(2)
C(4)–D(43)	1.08(2)	N–C(4)–D(41)	108(3)
		N–C(4)–D(42)	111(3)
		N–C(4)–D(43)	107(2)

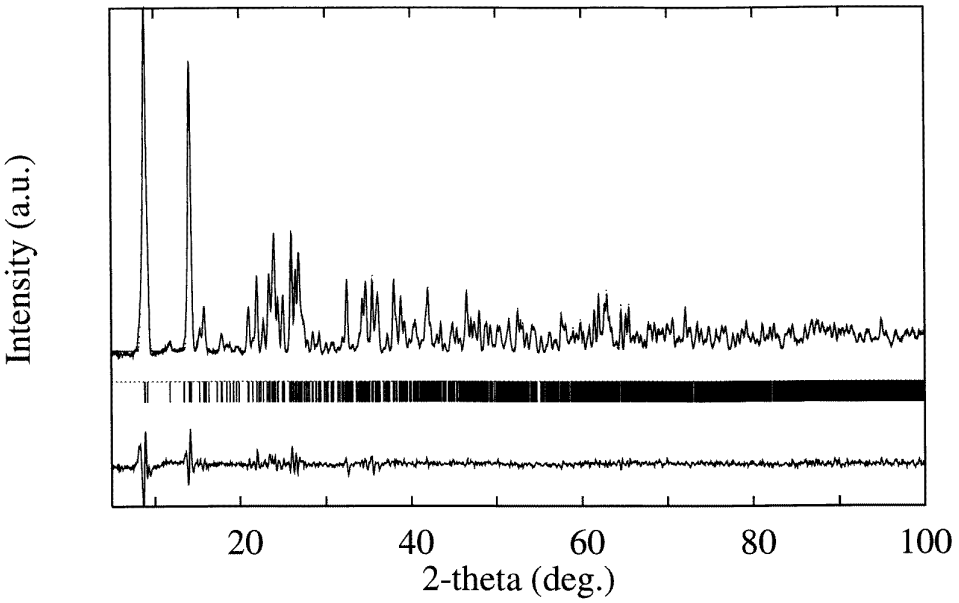

Figure 1. Neutron diffraction patterns of $N(CD_3)_4MnCl_3$ at 8 K in the ordered monoclinic phase. The observed profile is shown as dots and the calculated profile as a smooth curve; a difference profile is also presented. Short vertical markers represent reflections allowed by symmetry.

4.1. The two-site model

In this model [3, 11], the carbon atom C1 lies on the threefold axis of the site and the other three carbons C2, C3 and C4 are necessarily in a general position so as to form an

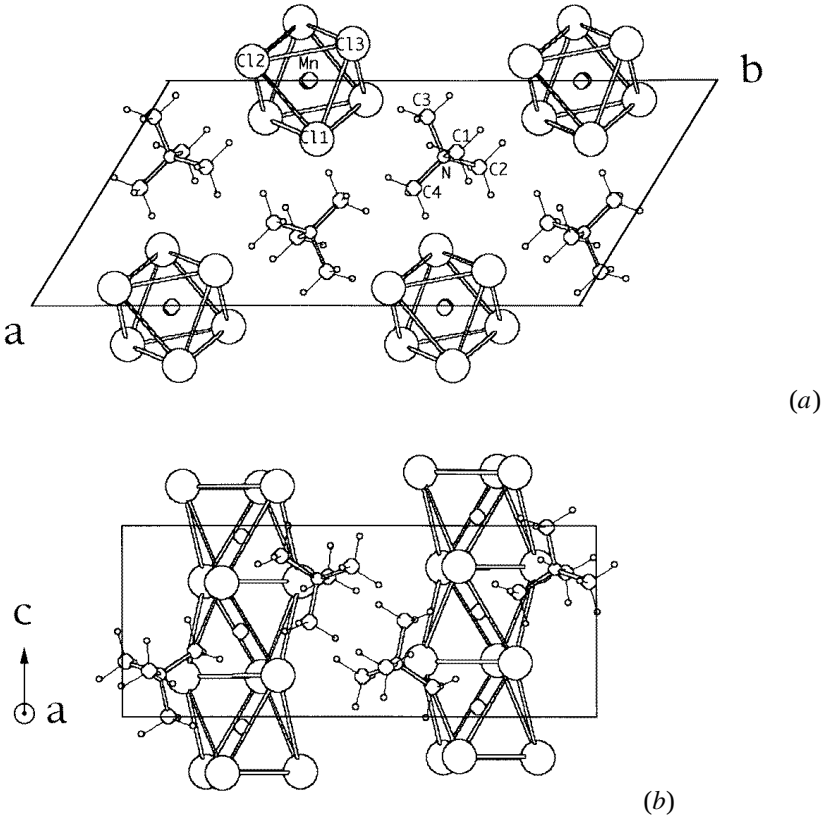

Figure 2. (a) Projection along c of the structure at 8 K. The deuterium atoms are not labelled for clarity of the plot. (b) Projection along a of the structure at 8 K. Note the antitranslational displacement of the octahedral chains along the c axis.

Table 3. Reliability factors of $N(CD_3)_4MnCl_3$ at 300 K in the disordered hexagonal phase. The e.s.d. of the last significant digit is given in parentheses.

Space group: $P6_3/m$ $(Z = 2)$	a(Å) = 9.142(3) c(Å) = 6.493(2)	
Two-site model	Three-site model	Six-site model
6 variables	8 variables	10 variables
R_{Bragg} (%) 17.6	R_{Bragg} (%) 14.1	R_{Bragg} (%) 12.7
R_{wp} (%) 8.49	R_{wp} (%) 7.43	R_{wp} (%) 7.06
$R_{expected}$ (%) 5.50 Wavelength (Å): 1.2266 Number of reflections: 413		

NC_4 tetrahedron. The other orientation is related by the horizontal mirror plane σ_h. Within this model, six parameters were refined including the chlorine position x/a and y/a on the mirror plane, one Euler angle for the TMA (about the C_3 axis) and two rotation angles for the CD_3 about their N–C bonds. A convergence process was quickly obtained which gave a rather high R_{Bragg} value of 17.6%.

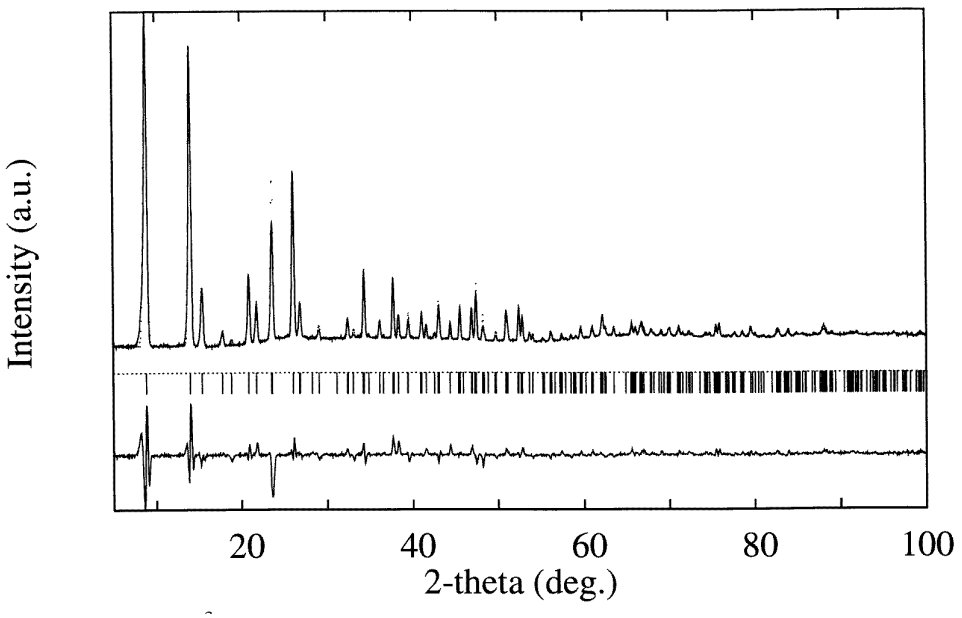

Figure 3. Neutron diffraction patterns of $N(CD_3)_4MnCl_3$ at 300 K in the disordered hexagonal phase. The observed profile is shown as dots and the calculated profile as a smooth curve; a difference profile is also presented. Short vertical markers represent reflections allowed by symmetry. One can note the oscillating background which is thought to be due to a large diffuse scattering [11].

4.2. The three-site model

This model was previously used in TMMC [11, 15] or the derived compound TMCB [21] but it leads to strongly distorted tetrahedra. As a matter of fact, these x-rays results gave satisfactory reliability factors to describe the mean distribution of electronic density of the organic group but do not provide us with a realistic picture since, as mentioned already, the tetrahedra were not observed to be strongly distorted by means of Raman scattering [8]. Therefore this model, which is compatible with the present phase transition $P6_3/m$ $(Z = 2) \Leftrightarrow P2_1/b$ $(Z = 4)$ of TMMC [13], has been reconsidered with NC_4 making a perfect tetrahedron. In this case, two carbons C1 and C2 located in a vertical plane are equivalent through the mirror plane σ_h and the last two carbons C3 and C4 lie on this mirror plane. In order to achieve the C_{3h} site symmetry, the other two orientations are deduced by rotation about the threefold axis. Within this model, eight parameters were refined including the chlorine position x/a and y/a on the mirror plane, one Euler angle for the TMA (about the C_3 axis) and four rotation angles of the CD_3 about their N–C bonds. The refinement converged toward a minimum which gave then a better R_{Bragg} value of 14.1%.

4.3. The six-site model

An alternative to these two models can be pictured in the light of the monoclinic structure. This alternative consists in a six-site model where the TMA are in instantaneous general positions [10, 23]. In particular, one can first imagine that the TMA orientation in the

Table 4. Atomic parameters of $N(CD_3)_4MnCl_3$ at 300 K (space group $P6_3/m$) obtained with the six-site model (see text) for rigid-body NC_4 groups. PP is the population parameter. The temperature factor has the form $\exp[-B\sin^2\theta/\lambda^2]$ where $B = 8\pi^2\langle u^2\rangle$. The estimated standard deviation (e.s.d.) of the last significant digit is given in parentheses. Each e.s.d. has been multiplied by a factor of 2.3 following [24].

Atom	Site	x	y	z	PP	B (Å^2)[a]
Mn	2b	0	0	0	1	2.5
Cl	6h	0.244(2)	0.147(2)	1/4	1	3.5
N	2c	1/3	2/3	1/4	1	2.5
C(1)	12i	0.313(1)	0.705(2)	0.469(2)	1/6	4
C(2)	12i	0.376(1)	0.817(2)	0.119(3)	1/6	4
C(3)	12i	0.172(2)	0.519(2)	0.176(3)	1/6	4
C(4)	12i	0.472(2)	0.626(2)	0.236(3)	1/6	4
D(11)	12i	0.253(2)	0.588(5)	0.555(5)	1/6	6
D(12)	12i	0.436(2)	0.789(4)	0.533(5)	1/6	6
D(13)	12i	0.237(2)	0.764(4)	0.473(4)	1/6	6
D(21)	12i	0.339(2)	0.897(5)	0.198(5)	1/6	6
D(22)	12i	0.510(2)	0.886(4)	0.091(4)	1/6	6
D(23)	12i	0.309(2)	0.775(4)	0.975(5)	1/6	6
D(31)	12i	0.074(4)	0.492(4)	0.288(5)	1/6	6
D(32)	12i	0.189(4)	0.411(4)	0.159(4)	1/6	6
D(33)	12i	0.139(4)	0.550(4)	0.030(4)	1/6	6
D(41)	12i	0.518(3)	0.645(4)	0.080(5)	1/6	6
D(42)	12i	0.573(3)	0.707(4)	0.339(4)	1/6	6
D(43)	12i	0.423(3)	0.495(4)	0.280(4)	1/6	6

[a] Fixed parameters.

monoclinic phase is simply one of those corresponding to the disordered hexagonal phase. Following this straightforward picture, one carbon C1 is placed above the mirror plane σ_h, not far away from the threefold axis. Another carbon C4 is located nearly on the same plane as the nitrogen. Then the last two carbons C2 and C3 are located below this latter plane in order to achieve the local instantaneous tetrahedral symmetry. In this way, the trial orientation of the TMA group (including the methyl rotation angles) for the refinement process was taken as that found in the monoclinic phase. The other five orientations are deduced from the C_{3h} site symmetry operations. Within this model, 10 parameters were refined including once again the chlorine position x/a and y/a on the mirror plane, three Euler angles for the NC_4 group and four rotation angles for the CD_3 about their respective N–C bonds. The refinement converged toward a minimum which gave a quite acceptable R_{Bragg} value of 12.7%. Given the complexity of the model and limitations inherent to powder diffraction data, it seemed to us not meaningful to go further in the refinement process. The refined parameters of the neutron diffraction pattern of $N(CD_3)_4MnCl_3$ at 300 K following this six-site model are summarized in table 4. In figure 3 we show a plot of the observed and calculated diffraction pattern and projections of the hexagonal structure are reported in figures 4(a) and 4(b).

5. Crystallographic description of the $P6_3/m \Leftrightarrow P2_1/b$ phase transition in $N(CD_3)_4MnCl_3$

As far as the octahedral chains are considered, it is found that the main change between the hexagonal and the monoclinic phase concerns anti-translational motions along the c axis;

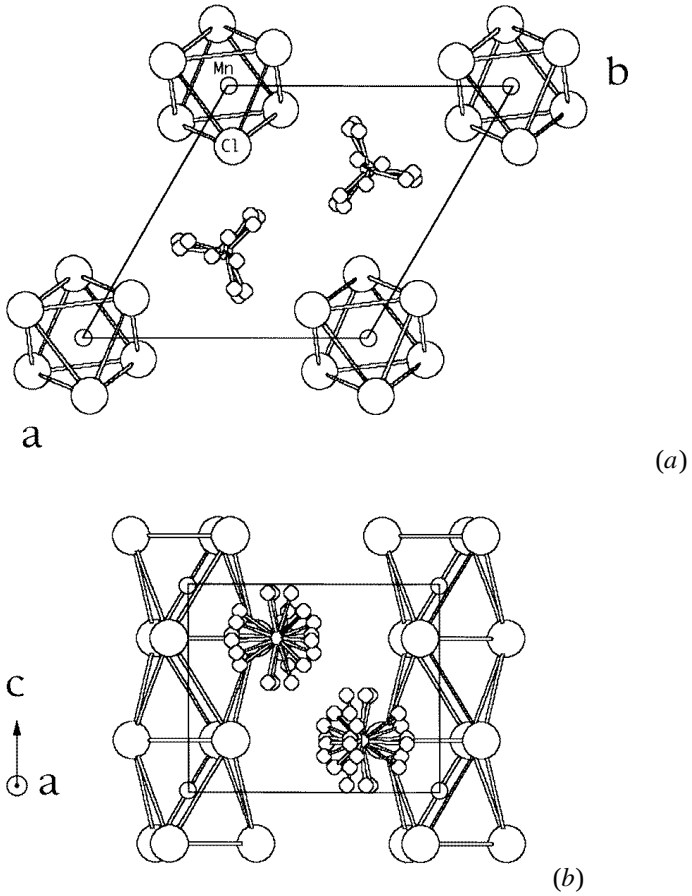

Figure 4. Projections of the structure at 300 K issuing from the 6W model (a) along *c* and (b) along *a*. The deuterium atoms are omitted for clarity of the plot.

as mentioned already, this motion is responsible for the doubling of the unit-cell along *b*. In fact, the chain displacement measured at 8 K along *c* with respect to its position in the hexagonal phase is quite large (see table 3), i.e. of the order of 0.25 Å. The TMA follow the anti-translational motions of the chain to a lesser extent: their displacement along *c* is about 0.17 Å. These observations nicely describe the transverse acoustic mode at point M $(0 \quad 1/2 \quad 0)$ of the hexagonal Brillouin zone [16] which was suspected to be related to the transition mechanism [10–13, 16]. It should be also pointed out that both TMA and octahedral chains are practically not translated in directions other than *c*, with respect to the hexagonal phase (see tables 1 and 4). At this point, it is worth noting that we have also tested another possible solution for the monoclinic phase, where the chains are not translated, i.e. where the manganese atoms form two families situated on inversion centres [8]; all attempts made in this way failed to reach a convergence into a stable solution and to give acceptable reliability factors. In fact, Braud *et al* [11] had already checked this possibility and the analysis of x-ray Patterson maps made it possible to conclude unambiguously that the manganese are in general position 4e. The data reported in tables 1 and 2 also show that the octahedra themselves are markedly distorted from their trigonal configuration in

the hexagonal phase as a result of the loss of the inversion symmetry; this situation agrees completely with the strong splittings (about 6% of the absolute frequency) of the octahedral degenerate bending modes (E_{2g} symmetry in the hexagonal phase) observed in the Raman spectra of the monoclinic phase [8, 10, 12]. So we conclude that the common picture [5] according to which the octahedral chains are practically unaffected by the phase transition of TMMC at 126 K is not correct.

Another point of interest concerns the rotational motion of the chains about the c axis; as a matter of fact, it is connected with the order parameter for the high-temperature second-order phase transition occurring at 389 K from $P6_3/m$ to $P6_3/mmc$ space group [11–13]. As can be deduced from tables 1 and 3, the octahedral chains have not rotated (to within 1 degree) around c. This result supports the idea [13] that the order parameter for the high-temperature transition is 'saturated' in the temperature range below 300 K; in other words, the transition at 389K is disconnected from that at 126 K.

The striking features of the TMA can be drawn as follows. Firstly, the structural refinement at 8 K indicates that the TMA internal conformation remains very close to that of the free molecule [22] even at very low temperature (see figure 5(a) and table 2). This result is clearly in agreement with previous Raman scattering experiments [8] and with the common picture of TMA behaving rather like a 'hard' molecular group. Secondly, it is shown that the monoclinic phase at 8 K is characterized by an orientational ordering of the TMA where the frozen orientation of this latter group corresponds neither to the two-site model nor to the three-site model. As evidenced in figure 5(b), the N–C1 bond is not far from the direction of the c (monoclinic) axis, so that a rotation by $\approx 17^\circ$ of the TMA is necessary to bring this group onto one of the orientations of the two-site model; on the other hand, a rotation of the TMA of roughly 10 degrees about the N—C4 bond will bring two carbons on the same horizontal plane, which is one of the possible orientations of the three-site model.

Therefore there arises the question of what kind of site and how many sites can be reasonably expected in the disordered hexagonal phase I. In accordance with the conclusions of Guillaume *et al* from incoherent quasielastic neutron scattering studies of TMMC [14], we can exclude the situation of an isotropic reorientation of the TMA. Furthermore torsional oscillations τ_{CH_3} around 220 and 300 cm^{-1} have been observed at room temperature by means of incoherent inelastic neutron scattering experiments [25], showing that the methyl groups are not in free rotation around the N–C bonds. Thus, it can be safely concluded that the carbon and the deuterium atoms in the hexagonal phase occupy statistically a finite number of well defined sites. Following this picture, we have tried to model the TMA orientational disorder distributed either in two or three sites with the constraint that the molecular symmetry is always T_d. Clearly, neither the two-site model nor the three-site model are satisfactory although this latter seems to be a better solution (see table 3). Therefore, the position of the TMA found in the monoclinic phase was supposed to be one of the six possible orientations in the hexagonal phase so as to achieve statistically the C_{3h} site symmetry. The reliability factors were found to be better than for the last two solutions and it turns out that the refined orientation of the TMA in the selected site coincides, within the experimental accuracy, to that of the frozen one in the monoclinic phase II, as it should be according to the picture of a Frenkel model. Of course, one can note that the reliability factors are improved as the number of sites increase but with a cost of no more than two to four parameters (see table 3). However, it could be pointed out that this solution found for the six-site model constitutes some compromise between the two-site and the three-site model. Indeed, one carbon C3 (see table 4) is located practically at the same place as those of the two-site model i.e. out of the threefold axis at height $z/c = 0.17$; the carbon C4

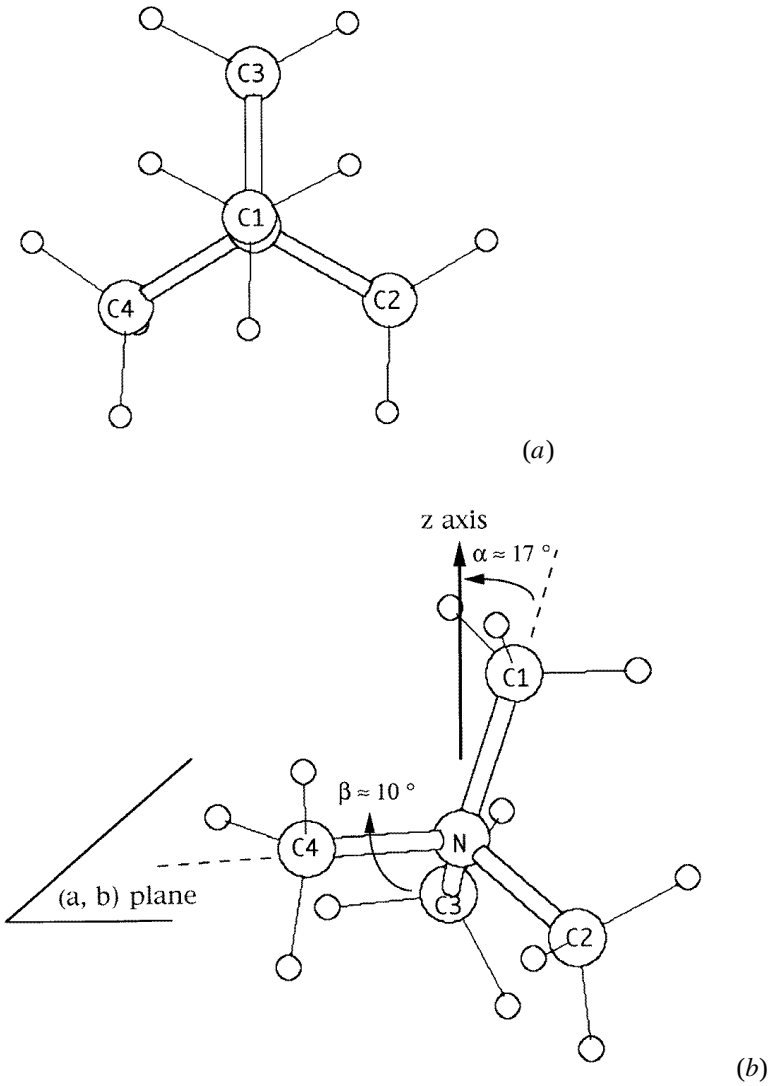

Figure 5. (a) Conformation of an isolated tetramethylamonium group obtained from the refinement of the ordered monoclinic phase. Note that the T_d molecular symmetry is nearly respected by the methyl positions although they were free from internal rotation about their N–C axis. (b) TMA orientation in the monoclinic phase. Its position corresponds to a general orientation nearly half way between the two-site and the three-site position.

situated very close to the mirror plane σ_h at $z/c = 0.25$ gives approximatively half the nuclear density distribution of the two carbons from the three-site model which lie in this mirror plane. The positions of carbons C1 and C2 could be compatible with both models if high Debye–Waller factors were introduced; a similar situation has been encountered in the structure determination of the hexagonal phase of TMCB [23].

In other words, and as a concluding remark, we have to keep in mind that, even though the six-site model provides a satisfactory description of the order/disorder process in TMMC, the structural refinement of the disordered phase must be considered with care, given

the inherent limits of powder diffraction techniques, the quality of the diffraction pattern, etc. Moreover, we have attempted to describe the mean TMA nuclear density distribution with the assumption of well localized sites within the Debye–Waller approximation, i.e. a harmonic one, which obviously constitutes also quite a rough approximation of the dynamical behaviour of the disordered hexagonal phase.

6. Conclusion

From the present neutron diffraction experiments on $N(CD_3)_4MnCl_3$, it is found that the $P6_3/m \Leftrightarrow P2_1/b$ phase transition is characterized by an anti-translational displacement of the octahedral chains and of the TMA groups along the *c* direction corresponding to the 'freezing' of the zone boundary transverse acoustic mode at point M of the Brillouin zone. We have attempted to model the orientational disorder of the TMA which 'is a proviso' for a better understanding of the phase transition mechanism of TMMC. Two main points emerge from this description. First, the conformation of the TMA in the ordered phase at low temperature remains very close to that of the free molecule with point group symmetry T_d [8, 12]. Second, the 'frozen' orientation of the TMA found in the ordered phase II seems to coincide with one out of the six energetically equivalent orientations in the hexagonal phase; in a Frenkel type description of disorder processes, this leads to the most general six-site model where the TMA occupy instantaneous general positions.

References

[1] Hutchings M T, Shirane G, Birgeneau R J and Holt S L 1972 *Phys. Rev.* B **5** 1999
[2] Boucher J P, Mezei F, Regnault L P and Renard J P 1985 *Phys. Rev. Lett.* **55** 1778
[3] Morosin B and Graeber E J 1967 *Acta Cryst.* **23** 766
[4] Morosin B 1972 *Acta Cryst.* B **28** 2303
[5] Peercy E T, Morosin B and Samara G A 1973 *Phys. Rev.* B **8** 3378
[6] Mangum B W and Utton D B 1972 *Phys. Rev.* B **6** 2790
[7] Tsang T and Utton D B 1976 *J. Chem. Phys.* **64** 3780
[8] Mlik Y, Daoud A and Couzi M 1979 *Phys. Status Solidi* a **52** 175
[9] Mlik Y and Couzi M 1982 *J. Phys. C: Solid State Phys.* **15** 6891
[10] Couzi M and Mlik Y 1986 *J. Raman Spectrosc.* **17** 117
[11] Braud M N, Couzi M, Chanh N B, Courseille C, Gallois B, Hauw C and Meresse A 1990 *J. Phys.: Condens. Matter* **2** 8209
[12] Braud M N, Couzi M, Chanh N B and Gomez-Cuevas A 1990 *J. Phys.: Condens. Matter* **2** 8229
[13] Braud M N, Couzi M and Chanh N B 1990 *J. Phys.: Condens. Matter* **2** 8243
[14] Guillaume F, Couzi M and Bée M 1992 *Physica* B **180 & 181** 714
[15] Jewess M 1982 *Acta Cryst.* B **38** 1418
[16] Hutchings M T, Pawley G S and Stirling W G 1983 *J. Phys. C: Solid State Phys.* **16** 115
[17] Young R A (ed) 1993 *The Rietveld Method* (Oxford: International Union of Crystallography, Oxford University Press)
[18] Rodriguez-Carvajal J 1990 *Abstract Satellite Meeting on Powder Diffraction 15th Congr. Int. Union Crystallogr. (Toulouse, 1990)* p 127
[19] Rodriguez V and Rodriguez-Carvajal J *J. Appl. Crystallogr.* submitted
[20] Dupas C and Renard J P 1973 *Phys. Lett.* **43A** 119
[21] Vis B, Chau C K, Weinstock H and Dietz R E 1974 *Solid State Commun.* **15** 1765
[22] Schlenkrich M 1992 *PhD Thesis* Darmstadt p 49
[23] Aguirre-Zamalloa G, Madariaga G, Couzi M and Breczewski T 1993 *Acta Cryst.* B **49** 691
[24] Bérar J F and Lelann P 1991 *J. Appl. Crystallogr.* **24** 1
[25] Guillaume F and Couzi M 1992 unpublished